Cadmium adsorption by coal combustion ashes-based sorbents—Relationship between sorbent properties and adsorption capacity

Marco Balsamo[a], Francesco Di Natale[a], Alessandro Erto[a], Amedeo Lancia[a], Fabio Montagnaro[b,*], Luciano Santoro[b]

[a] *Dipartimento di Ingegneria Chimica, Università degli Studi di Napoli Federico II, Piazzale Vincenzo Tecchio 80, 80125 Napoli, Italy*
[b] *Dipartimento di Chimica, Università degli Studi di Napoli Federico II, Complesso Universitario di Monte Sant'Angelo, 80126 Napoli, Italy*

ARTICLE INFO

ABSTRACT

A very interesting possibility of coal combustion ashes reutilization is their use as adsorbent materials, that can also take advantage from proper beneficiation techniques. In this work, adsorption of cadmium from aqueous solutions was taken into consideration, with the emphasis on the intertwining among waste properties, beneficiation treatments, properties of the beneficiated materials and adsorption capacity. The characterization of three solid materials used as cadmium sorbents (as-received ash, ash sieved through a 25 μm-size sieve and demineralized ash) was carried out by chemical analysis, infrared spectroscopy, laser granulometry and mercury porosimetry. Cadmium adsorption thermodynamic and kinetic tests were conducted at room temperature, and test solutions were analyzed by atomic absorption spectrophotometry. Maximum specific adsorption capacities resulted in the range 0.5–4.3 mg g^{-1}. Different existing models were critically considered to find out an interpretation of the controlling mechanism for adsorption kinetics. In particular, it was observed that for lower surface coverage the adsorption rate is governed by a linear driving force while, once surface coverage becomes significant, mechanisms such as the intraparticle micropore diffusion may come into play. Moreover, it was shown that both external fluid-to-particle mass transfer and macropore diffusion hardly affect the adsorption process, which was instead regulated by intraparticle micropore diffusion: characteristic times for this process ranged from 4.1 to 6.1 d, and were fully consistent with the experimentally observed equilibrium times. Results were discussed in terms of the relationship among properties of beneficiated materials and cadmium adsorption capacity. Results shed light on interesting correlations among solid properties, cadmium capture rate and maximum cadmium uptake.

© 2011 Elsevier B.V. All rights reserved.

1. Overview

Among the fossil sources employed to satisfy the ever-increasing world energy demand, coal is becoming more and more important due to social, political and economical reasons. Consequently, many hundreds of Mton y^{-1} of *coal combustion ash* (CCA) are produced worldwide, and particular attention must be paid to landfill disposal of this residue, a management option that must be limited in accordance with the issuing of recent specific regulations. In this framework, any proposal aimed at employing this industrial waste should be carefully considered [1–3]. One of the main fields of CCA reuse is the cement and concrete industry [4] but, when this option is not economically convenient, alternative applications have to be searched for. In this context, *adsorption* can represent an interesting option. In fact, coal (mainly fly) ashes can

be used as sorbent to replace the traditionally employed activated carbons (characterized by high investment and regeneration costs) as they show a moderately porous structure and the presence of both an inorganic matrix and unburned carbon which are involved in the pollutants removal from liquid and gaseous effluents [5–10]. Although raw CCA are sometimes employed as sorbents, in many cases it is useful to beneficiate them by means of different *activation treatments* aimed at improving their physical, chemical and morphologic characteristics to increase their selectivity toward specific pollutants. Examples of these techniques are: (i) *mechanical sieving* of CCA particles, which allows to select and exploit the different physico-chemical properties of specific size ranges; (ii) *demineralization by acid attack*, which is aimed at increasing CCA carbon content by removing its mineral fraction. Other beneficiation methods have been proposed, such as basic treatments, pyrolysis and CO_2/steam gasification [11–14].

Heavy metals can be dangerously present in industrial waste streams such as those generated by, *e.g.*, metal extraction, mine drainage, paint/ink manufacture processes, operations concerning

Nomenclature

C	cadmium concentration in the liquid solution after adsorption [mg L^{-1}]
C_0	cadmium initial concentration in the liquid solution [mg L^{-1}]
D_0	cadmium diffusivity in water [m^2 s^{-1}]
D_{eff}	cadmium effective diffusivity [m^2 s^{-1}]
D_{macro}	cadmium diffusivity in macropores [m^2 s^{-1}]
D_{micro}	cadmium diffusivity in micropores [m^2 s^{-1}]
d_S	mean Sauter particle size [m]
h	initial adsorption rate [mg g^{-1} min^{-1}]
$k_{kin,1}$	specific kinetic constant for the pseudo-first-order kinetic model (Eq. (2)) [min^{-1}]
$k_{kin,2}$	specific kinetic constant for the pseudo-second-order kinetic model (Eq. (3)) [g mg^{-1} min^{-1}]
m	sorbent amount [g]
q	specific adsorption capacity [mg g^{-1}]
q_{max}	maximum q-value obtained from kinetic tests [mg g^{-1}]
R	specific Boltzmann universal constant [J K^{-1}]
r_P	adsorbent mean pore radius [m]
Sh	Sherwood no.
T	temperature [K]
t	adsorption time [min]
V	volume of the cadmium aqueous solution [L]

Greek symbols

ΔG	free energy change [kJ mol^{-1}]
ε	particle porosity
λ	ratio Stokes–Einstein radius of the cadmium ion/adsorbent mean pore radius
μ	water viscosity [kg m^{-1} s^{-1}]
τ	pores tortuosity
τ_{ext}	characteristic time for external mass transfer [s]
τ_{macro}	characteristic time for macropore diffusion [s]
τ_{micro}	characteristic time for micropore diffusion [s]

Table 1
CCA chemical composition and proximate analysis (dry basis) (wt%).

Chemical composition	wt%
CaO	4.25
SO$_3$	n.d.
Al$_2$O$_3$	21.80
SiO$_2$	34.20
MgO	1.03
Na$_2$O	0.55
K$_2$O	0.96
TiO$_2$	1.49
Fe$_2$O$_3$	7.24
Loss on ignition	26.70
Total	98.22

Proximate analysis (dry basis)	wt%
Volatiles	3.68
Fixed carbon	22.26
Ashes	74.06
Total	100.00

ceramics, cosmetic, electrogalvanization, fertilizers, pharmaceutical, pesticides, pulp/paper and textile industries. It is well known that many heavy metals, when present in high amount in effluents, are dangerous for both the human health and the environment. In fact, they are generally non-biodegradable (thus, very stable and persistent), characterized by high toxicity, and usually recognized to have carcinogenic properties. One particular hazard related to such compounds is their tendency to bioaccumulate in the food chain, thus being assimilated in the living tissues. Therefore, the removal of metal compounds from natural waters and wastewater streams is an issue of great environmental relevance. While in some cases methods such as chemical oxidation/reduction, chemical precipitation, electrochemical treatment, filtration, ion exchange, reverse osmosis and solvent extraction can be employed for heavy metals removal, in many cases adsorption is preferred since it is economical, effective, simple, versatile and suitable when, as often it is, the metal concentration in the wastewater is very low [15–31].

In this work, the adsorption capacity of a heavy metal, namely *cadmium*, on raw CCA- and beneficiated CCA-based sorbents has been investigated. Although many papers can be found in the literature on the possibility of removing heavy metals from wastewaters by adsorption on low-cost materials, the intertwining among waste properties, beneficiation treatments, properties of the beneficiated materials and adsorption capacities has been only partly elucidated [9,30]. While in a previous work [30] the attention was mainly devoted to the removal of dyes (only an equilibrium study concern-

ing the system cadmium/raw CCA was reported), the aim of this paper is to investigate, from a thermodynamic and kinetic point of view, the cadmium adsorption capacity of CCA both as-received and after beneficiation by either mechanical sieving or demineralization, since these techniques are both aimed at enhancing the carbon content and/or the porosity of the adsorbent material [30,32].

2. Experimental

2.1. Properties of the raw coal combustion ash and sorbents characterization techniques

The coal combustion fly ash utilized in this work comes from an Italian power plant operated by Enel; CCA chemical composition and proximate analysis are reported in Table 1. It can be observed the presence of a significant silico-aluminous fraction (though iron and calcium were detected in non-negligible amounts) and, more generally, an ash content of nearly 74%. The CCA fixed carbon content was about 22%, a value justified by the very nature of this material (fly ash), which could imply short mean residence times (and, therefore, uncompleted carbon conversion degree) into the combustor.

The adsorbent materials employed in this study were further characterized by the following techniques: (i) X-ray fluorescence, performed by a Bruker Explorer S4 analyzer; (ii) infrared spectroscopy, carried out by a FTIR 430 Jasco spectrometer operated in the wavenumbers range 400–4000 cm^{-1}; (iii) laser granulometric analysis, performed by a Malvern Instruments Master Sizer 2000 granulometer operated down to a minimum particle size of 0.02 μm; (iv) porosimetric analysis, carried out by a mercury intrusion Thermo Finnigan Pascal 240/140 porosimeter operated in the pore size range 3.7–1000 nm.

2.2. Beneficiation treatments

Starting from CCA, two other different sorbents were obtained through beneficiation treatments. The first one (termed F25) was produced by sieving raw CCA through a 25 μm-size sieve. Indeed, as it will be shown in the results, almost 50% of CCA particles is finer than 25 μm, and this less-than-25 μm fraction was chosen in order to have a material with a smaller mean diameter than CCA. The second one (termed DEM) derived from raw CCA demineralization by HCl/HF attack, as described elsewhere [30]. It is recalled here that Al- and Si-based compounds are essentially removed by HCl and HF solutions, respectively. This demineralization treatment

determined very acidic conditions when DEM is kept in contact with water: therefore, demineralization was followed by a neutralizing treatment with NaOH solution (pH 9; liquid/solid ratio = 0.35 L g^{-1}) washing.

2.3. Adsorption tests

Cadmium adsorption thermodynamic and kinetic tests were conducted at room temperature using, alternatively, CCA, F25 and DEM as adsorbents. Thermodynamic tests were aimed at evaluating the adsorption isotherms: to this end, a sorbent amount of 1 g was contacted in a stirred glass beaker with an aqueous solution having volume of 0.1 L and cadmium initial concentration ranging from 5 to 50 mg L^{-1} (reagent grade Cd(NO$_3$)$_2$·4H$_2$O). Preliminary tests indicated that an adsorption time of 6 d, 4 d and 15 min (for CCA, F25 and DEM, respectively) was needed to reach equilibrium conditions. Kinetic tests were conducted, by holding the other operating conditions, for times ranging from 15 min to 7 d and using a cadmium initial concentration of 50 mg L^{-1}. This concentration value was chosen as representative of typical loads shown by cadmium-contaminated industrial waste streams; values on the order of 50 mg L^{-1} were often reported in the related literature [14,16,20,23,24]. Preliminary tests indicated that, in the presence of raw CCA, the equilibrium cadmium solution pH equaled to 12 (the value of the pH of the point of zero charge was equal to 9). These strong alkaline properties should be likely related to calcium ions leaching: it can be verified, in fact, that even if the CaO concentration in the raw ash is 4.25 wt% (as reported in Table 1), this value is able to mainly justify the pH-value experimentally observed. A similar scenario was verified for F25, that did not show significant variations in the chemical composition with respect to CCA, as set forth in the results. These operating conditions would strongly affect cadmium adsorption, since species such as Cd(OH)$_2$ would likely precipitate: therefore, an experimental campaign devoted to investigate the influence of equilibrium pH on equilibrium cadmium adsorption capacity was carried out. These results suggested to operate at equilibrium pH around 7.5, value at which the equilibrium cadmium adsorption capacity resulted as optimal. To this end, the initial cadmium solution pH was adjusted with HNO$_3$ (0.1 M) and NaOH (0.025 M) solutions, in order to obtain an equilibrium pH around 7.5 for all the tests. In particular, HNO$_3$ was employed in the case of both CCA and F25 (showing alkaline properties, as previously discussed), while NaOH was used in the case of DEM, which presents an acid behaviour due to the intrinsic acid demineralization treatment suffered by this material (in particular, in the presence of untreated DEM, the equilibrium solution pH equaled to 2). Since for any kinetic test the solution pH practically reached its equilibrium value over a time scale shorter than that characteristic for the kinetic tests, it is believed that the pH kinetic evolution from the initial to the equilibrium value does not affect the adsorption results, at least under the conditions explored in this work.

After each test, liquid solutions were filtered and analyzed by atomic absorption spectrophotometry (employing a Varian SpectrAA 220 apparatus), in order to determine the pollutant concentration and, therefore, the specific adsorption capacity by means of the material balance:

$$q = \frac{(C_0 - C)V}{m} \tag{1}$$

2.4. Adsorption kinetics models

The most diffused models for the interpretation of adsorption kinetics data are the pseudo-first-order model of Lagergren (Eq. (2)) and the pseudo-second-order model of Ho and McKay (Eq. (3))

[33,34]:

$$\frac{dq(t)}{dt} = k_{kin,1}[q_{max} - q(t)]; \quad \underline{\underline{B.C.}} \quad q(0) = 0 \tag{2}$$

$$\frac{dq(t)}{dt} = k_{kin,2}[q_{max} - q(t)]^2; \quad \underline{\underline{B.C.}} \quad q(0) = 0 \tag{3}$$

The solutions of Eqs. (2) and (3), in their linearized forms, read, respectively:

$$\ln\left[\frac{q_{max} - q(t)}{q_{max}}\right] = -k_{kin,1}t \tag{4}$$

$$\frac{t}{q(t)} = \frac{1}{k_{kin,2}q_{max}^2} + \frac{t}{q_{max}} \tag{5}$$

If experimental data follow either the first- or the second-order model, they must obey to linear functions once the respective LHS of Eqs. (4) and (5) is plotted against t: this also allows to estimate the values of the kinetic constants. For several practical applications, the initial adsorption rate is a relevant parameter, too. It can be computed from experimental data as:

$$h = \left.\frac{dq(t)}{dt}\right|_{t=0} \tag{6}$$

Moreover, the experimental kinetic results allow the estimation of a characteristic adsorption time that can be compared with the characteristic times for (i) external fluid-to-particle mass transfer (τ_{ext}), (ii) macropore (τ_{macro}) and (iii) micropore (τ_{micro}) diffusion [35]. By assuming the adsorbent particles as equal spheres having as diameter the mean Sauter particle size, and under the assumptions of the classical penetration theory, it is:

$$\tau_{ext} = \frac{d_S^2}{4Sh^2D_0} \tag{7}$$

$$\tau_{macro} = \frac{(d_S/4)^2}{D_{macro}} \tag{8}$$

$$\tau_{micro} = \frac{(d_S/4)^2}{D_{micro}} \tag{9}$$

In Eq. (7), $D_0 = 1.89 \times 10^{-9}$ m^2 s^{-1} [36]. In Eq. (8), D_{macro} can be calculated as [37]:

$$D_{macro} = D_0 \frac{\varepsilon}{\tau} \frac{1}{(1-\lambda)^2}\left(1 + \frac{9}{8}\lambda \ln \lambda - 1.539\lambda\right) \tag{10}$$

where τ is taken as ε^{-1} [38] and the parameter λ can be calculated as [37]:

$$\lambda = \frac{RT}{6\pi\mu D_0 r_P} \tag{11}$$

On the contrary, estimations for D_{micro} are more complex to obtain from literature, even though its order of magnitude is expected to range in the interval 10^{-17}–10^{-19} m^2 s^{-1} [35,39]. In this paper, the experimental data are also analyzed in the light of the Reichenberg equation [14,40,41], to find out whether the adsorption kinetics should be related to macropore or micropore diffusion:

$$\ln\left[1 - \left(\frac{q(t)}{q_{max}}\right)^2\right] = -\frac{4\pi^2 D_{eff}}{d_S^2}t \tag{12}$$

If this model is valid, by plotting as a linear function the LHS of Eq. (12) against t it is possible to estimate D_{eff} that can be eventually compared with D_0 and D_{macro} to find out the controlling mechanism.
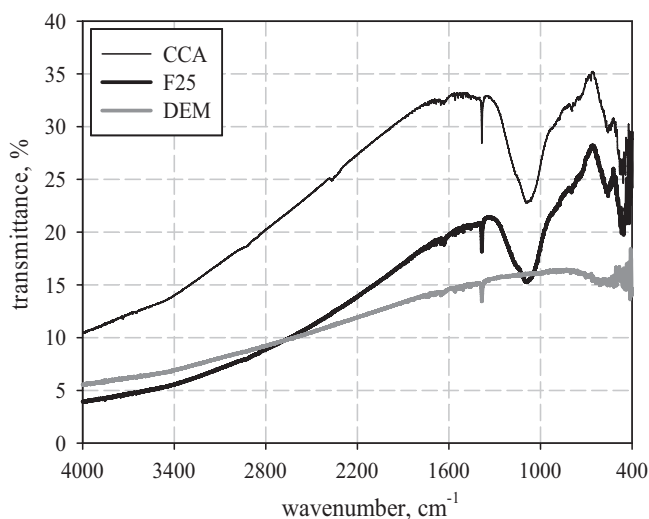
Fig. 1. Infrared spectroscopy results for CCA, F25 and DEM.

Table 2
Relevant parameters, both experimentally observed and theoretically derived, obtained in this study.

	F25	CCA	DEM
Carbon content (wt%)	22	22	93
d_S (μm)	3	10	15
Cumulative pore volume (mm^3 g^{-1})	148.8	69.5	62.4
ΔG (kJ mol^{-1})	−28.5	−26.6	−20.8
Equilibrium constant (L mg^{-1})	0.87	0.41	0.04
q_{max} (mg g^{-1})	4.3	2.0	0.5
$k_{kin,1}$ (min^{-1})	1.0×10^{-3}	7.2×10^{-4}	–
$k_{kin,2}$ (g mg^{-1} min^{-1})	3.6×10^{-4}	3.0×10^{-4}	–
h (mg g^{-1} min^{-1})	4.3×10^{-3}	1.4×10^{-3}	–
τ_{ext} (s)	$\ll 1$	$\ll 1$	$\ll 1$
D_{macro} (m^2 s^{-1})		7.15×10^{-11}	
τ_{macro} (s)	8×10^{-3}	9×10^{-2}	2×10^{-1}
D_{micro} (m^2 s^{-1})	1.6×10^{-18}	1.2×10^{-17}	–
τ_{micro} (d)	4.1	6.1	–
Equilibrium time[a] (d)	4	6	–

[a] Value estimated from experiments.

3. Results and discussion

3.1. Adsorbents characterization

CCA, F25 and DEM adsorbents were characterized by infrared spectroscopy, laser granulometry and mercury porosimetry. Fig. 1 shows the infrared spectroscopy results for CCA, F25 and DEM. In all spectra a peak centered at 1383 cm^{-1} was revealed, mainly ascribable to inorganic carbonate structures [42,43]. The reduced peak intensity for DEM material should be related to its limited inorganic content, as set forth in this paragraph. The circumstance that the DEM spectrum appears lacking in other peaks is instead due to the high carbon content of this ash-derived material, likely characterized by a graphitic structure (because of the high temperatures experienced by the parent material into the combustor) not showing infrared bands [44]. On the other hand, the peaks evolution at wavenumbers smaller than 1300 cm^{-1} do mirror the silico-aluminous structure for both CCA and F25, and they are a clue of the non-significant chemical modifications induced by the sieving treatment. More in detail, the peaks centered at 1090, 560 and 460 cm^{-1} are related to the asymmetric stretching of Al,Si–O groups, the presence of aluminium in aluminosilicates such as mullite and the Si–O–Si bending, respectively [cf. 45]. Relevant parameters concerning granulometric and porosimetric results are listed in Table 2. CCA showed a d_S-value of 10 μm, a d_{50}-value (the particle diameter for which 50 wt% of the material is finer and 50 wt% is coarser) of 25 μm and a d_{90}-value of 70 μm. Moreover, particles coarser than 150 μm were substantially absent, in line with other results reported in the pertinent literature [10,16]. As expected, the F25 sorbent was characterized by finer particle sizes ($d_S = 3$ μm); differently, the demineralization treatment ended up in a moderate increase of the mean particle size ($d_S = 15$ μm), possibly related to the larger size of carbon particles constituting most of the DEM material. Porosimetric analysis revealed, in the pore size range investigated, the following cumulative specific pore volumes: 148.8 mm^3 g^{-1} (F25), 69.5 mm^3 g^{-1} (CCA), 62.4 mm^3 g^{-1} (DEM). In particular, the textural characterization of the raw ash indicated that the 8.1%, 8.6%, 26.6% and 56.7% of the porosity lies in the range 3.7–10, 10–100, 100–500 and 500–1000 nm, respectively, thus evidencing a prevailing macroporous structure for the raw sorbent. As a general consideration, porosity values were in any case comparable with those reported in the literature for coal ash-based adsorbents [7,9]. Moreover, the two beneficiation treatments resulted into different effects on the sample porosity: it increased

(about 2 times) when CCA was sieved into F25, and moderately decreased when CCA was subjected to demineralization, that can be possibly ascribed to the physico-chemical modifications induced by the acid treatments. Finally, it is noted that mechanical sieving did not induce any significant change neither in the carbon content of the solid material (which thus was again around 22%) nor in its chemical composition (actually, with respect to CCA, only a moderate increase in the SiO$_2$ content – from 34.20 to 38.00 wt% – and a moderate decrease in the Fe$_2$O$_3$ amount – from 7.24 to 5.89 wt% – was observed), while the resulted DEM carbon content equaled to about 93%, showing that the demineralization treatment was very effective in depleting CCA of its inorganic fraction (Table 2).

3.2. Thermodynamic tests for cadmium adsorption on CCA, F25 and DEM

The adsorption isotherms of cadmium on CCA, F25 and DEM are reported in Fig. 2. They can be classified as Langmuir-type curves,
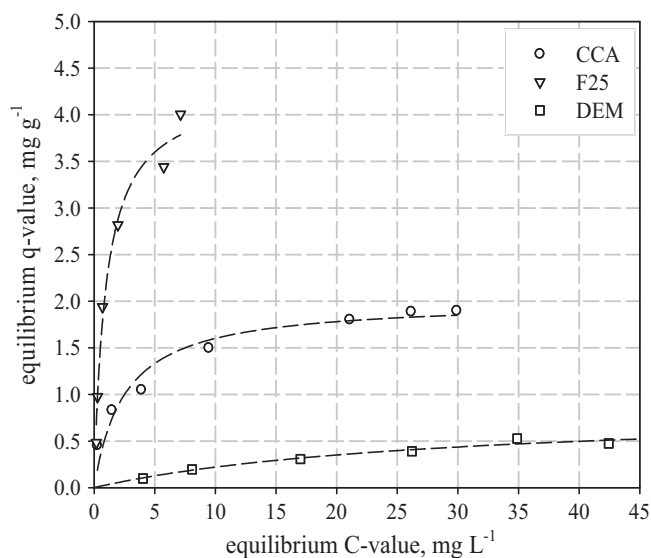

Fig. 2. Adsorption isotherms for cadmium adsorption on CCA, F25 and DEM (sorbent amount = 1 g; liquid solution volume = 0.1 L; adsorption time = 6 d, 4 d and 15 min for CCA, F25 and DEM, respectively). Dashed lines indicate the fittings according to the Langmuir model.
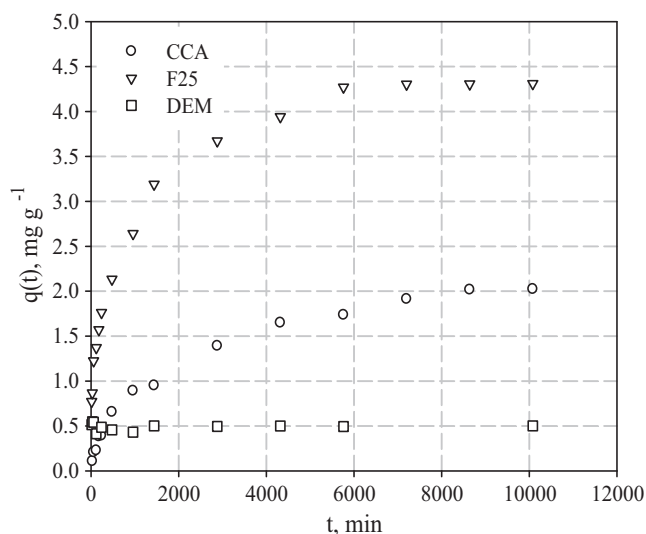
Fig. 3. Kinetic tests for cadmium adsorption on CCA, F25 and DEM: plots of the specific adsorption capacity versus time (sorbent amount = 1 g; liquid solution volume = 0.1 L; cadmium initial concentration = 50 mg L^{-1}).

Fig. 4. Fitting kinetic data according to the Ho and McKay model (Eq. (5)) for cadmium adsorption on CCA and F25: (a) whole *t*-range investigated; (b) enlargement for *t* < 500 min.

showing saturation conditions (monolayer) around equilibrium cadmium concentrations of 25, 7 and 42 mg L^{-1} and equilibrium specific adsorption capacities of 2, 4 and 0.5 mg g^{-1} for CCA, F25 and DEM, respectively. Moreover, manipulation of the equilibrium results according to the well-known Langmuir model (see Table 2) gives the following values for the equilibrium constant: 0.41 L mg^{-1} (CCA), 0.87 L mg^{-1} (F25) and 0.04 L mg^{-1} (DEM). This allows to calculate the following values for the process free energy change (at room temperature) ΔG: −26.6 kJ mol^{-1} (CCA), −28.5 kJ mol^{-1} (F25) and −20.8 kJ mol^{-1} (DEM), highlighting the spontaneous nature of the process and in line with the literature indication that ΔG is typically on the order of 10 kJ mol^{-1} for metal adsorption onto low-cost adsorbents [21,25,46–48]. Therefore, when comparing these data, a ranking F25 > CCA > DEM could be observed. Furthermore, it is recalled that the same literature above-referred indicates values of the process enthalpy change on the order of 10 kJ mol^{-1} (underlining the endothermic nature of adsorption) and values of the process entropy change on the order of 10–10^2 kJ mol^{-1} K^{-1} (suggesting an increased randomness at the solid–solution interface during adsorption).

Possible explanations for the trend F25 > CCA > DEM will be developed in the next section, that deals with kinetic tests. As reported in the Experimental, these tests were carried out at a cadmium initial concentration of 50 mg L^{-1}: in the light of the thermodynamic results, this value appears to be high enough to allow investigating the kinetic evolution of all the systems up to the adsorbents saturation conditions.

3.3. Kinetic tests for cadmium adsorption on CCA, F25 and DEM

Fig. 3 reports the results of the cadmium adsorption kinetic tests, using either CCA or F25 or DEM as sorbent and expressed in terms of $q(t)$ profiles (see Eq. (1)). For CCA and F25 sorbent, $q(t)$-values increased with time reaching an equilibrium value ($q_{max} \cong 2.0$ and 4.3 mg g^{-1}, respectively) after about 6 and 4 d, respectively. For DEM sorbent a completely different pattern was observed: in fact, it was almost saturated just after 15 min, the shortest adsorption time experienced in this work ($q_{max} \cong 0.5$ mg g^{-1}). It is highlighted that the q_{max}-values obtained from kinetic tests are in a very good agreement with the monolayer adsorption capacities obtained from the inspection of the adsorption isotherms (*cf.* Fig. 2). Due to the very
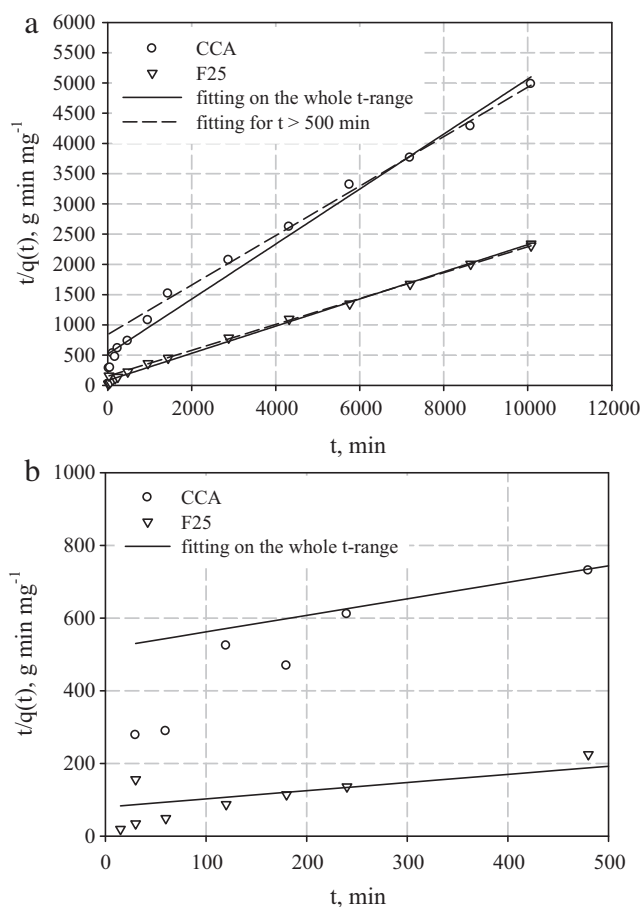
fast saturation of DEM, no fitting of kinetic data was possible for this sorbent, while the regressions of the experimental results for CCA and F25 are reported in Figs. 4 and 5.

Fig. 4 illustrates the fittings of kinetic data according to the Ho and McKay model (Eq. (5)): when (Fig. 4a) the regressions according to the solid lines are considered (namely, those performed over the whole *t*-range investigated), it can be observed that, although determination coefficient values were around 0.99 for both sorbents regression data analysis, large deviations from the experimental data (especially for the raw material) were experienced for the shortest adsorption times (*t* < 500 min, see Fig. 4b). In fact, for the statistical analysis, the experimental data at low independent variable (time) values have a negligible weight on the determination coefficient: hence, the latter should not be used as the only criterion for best fitting model individuation. As a consequence, the pseudo-second-order model can be reliably applied only for *t* > 500 min (Fig. 4a, dashed lines), yielding $k_{kin,2} = 3.0 \times 10^{-4}$ and 3.6×10^{-4} g mg^{-1} min^{-1} for CCA and F25, respectively (Table 2).

Fig. 5 shows the fittings of kinetic data according to the Lagergren model (Eq. (4)): as expected at this point (Fig. 5a), the regressions in solid lines failed to represent data for the longest adsorption times (*t* > 500 min), so this model was actually employed only to represent data for *t* < 500 min (Fig. 5b, dashed lines). Values for $k_{kin,1}$ and *h* equal to 7.2×10^{-4} min^{-1} and 1.4×10^{-3} mg g^{-1} min^{-1} (for CCA) and to 1.0×10^{-3} min^{-1} and 4.3×10^{-3} mg g^{-1} min^{-1} (for F25) were obtained, respectively (Table 2).
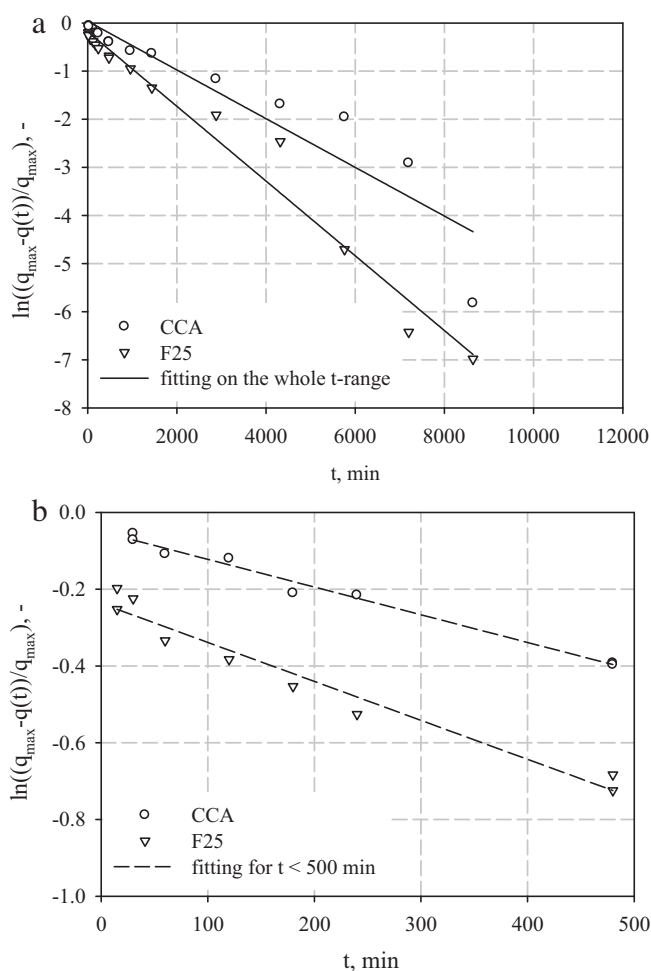
Fig. 5. Fitting kinetic data according to the Lagergren model (Eq. (4)) for cadmium adsorption on CCA and F25: (a) whole *t*-range investigated; (b) enlargement for *t* < 500 min.

Altogether, this shows that for lower surface coverage the adsorption rate is governed by a linear driving force $(q_{max} - q(t))$ which is typical of overall mass transfer controlling phenomena. Once surface coverage becomes significant (in this work, when $q(t)/q_{max}$ is around 0.3 and 0.5 for CCA and F25, respectively), different mechanisms tend to prevail, such as those related to the dishomogeneities of active sites on the heterogeneous surface of the ash, or to the occurrence of micropore diffusion controlling phenomena.

An analysis of the characteristic times of the involved processes now follows (relevant parameters are listed in Table 2). By letting $Sh = 2$, from Eq. (7) it is $\tau_{ext} \ll 1$ s for each sorbent investigated. By letting $R = 1.38 \times 10^{-23}$ J K^{-1}, $T = 298$ K, $\mu = 10^{-3}$ kg m^{-1} s^{-1} and $r_P \cong 10$ nm (an order of magnitude estimated from the porosimetric investigation), from Eq. (11) it is $\lambda = 0.0115$; when this value is used in Eq. (10), and for $\varepsilon \cong 0.2$ (again, from the porosimetric analysis), it is $D_{macro} = 7.15 \times 10^{-11}$ m^2 s^{-1} (then, about two order of magnitude smaller than D_0) and (Eq. (8)) $\tau_{macro} \cong 10^{-3}$–$10^{-1}$ s, depending on the sorbent. Therefore, both external fluid-to-particle mass transfer and macropore diffusion characteristic times are far shorter than the observed characteristic times of the process (around 5 d): this means that adsorption is likely to be regulated by intraparticle micropore diffusion. In order to give an estimation for τ_{micro}, kinetic results were worked out according to the Reichenberg Eq. (12) for CCA and F25. Fig. 6 reports the plots of the LHS of Eq. (12) *vs. t*, from
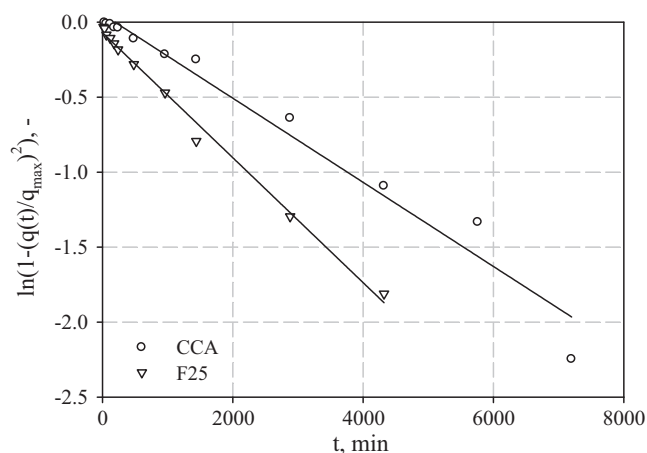

Fig. 6. Fitting kinetic data according to the Reichenberg model (Eq. (12)) for cadmium adsorption on CCA and F25.

which values for D_{eff} equal to 1.2×10^{-17} and 1.6×10^{-18} m^2 s^{-1} can be calculated for CCA and F25, respectively. It is $D_{eff} \ll D_0$, D_{macro}: therefore, it is actually $D_{eff} = D_{micro}$, and this appears to be consistent with former indication for sodium and calcium diffusion in soda-lime glass [39]. Finally, Eq. (9) allows to estimate $\tau_{micro} = 6.1$ and 4.1 d for CCA and F25, respectively. When these values are compared with the characteristic times required for $q(t)$ to closely approach q_{max} (*cf.* Fig. 3), it appears that τ_{micro} is very close to the equilibrium time for both the sorbents: this should underline the building-up of a micropore diffusion-controlled regime for the systems under investigation, and suggest that the Reichenberg approach can be a useful tool for estimating the characteristic time of the process for systems reaching saturation conditions not too fast.

As a general consideration, when the raw ash is sieved into F25, neither its carbon content nor its chemical composition substantially changes, but both the exposed contact surface ($6/d_S$) and the cumulative specific pore volume increase. On the other hand, when CCA is demineralized, the carbon content strongly increases but both contact surface and porosity moderately decrease, at least under the operating conditions adopted in this work. Therefore (*cf.* Table 2) a ranking F25 > CCA > DEM could be envisaged as far as both contact surface and porosity are concerned, and this ranking still holds when adsorption isotherms, q_{max}-values, CCA and F25 kinetic constants and initial adsorption rates are considered. This means that the demineralization treatment does not increase the cadmium removal but, instead, reduces its extent. This should be related to the observation that this treatment is bound up with changes in the physico-chemical/microstructural characteristics of the ash through the removal of the inorganic fraction and the generation of an oxidized sorbent matrix rich in carbon but having a smaller contact surface and porosity. On the other hand, cadmium adsorption on CCA appears to be favoured by the presence of the ash inorganic fraction together with a high contact surface and specific porosity. These insights should shed light on the relevance of adopting beneficiation treatments based on the improving of determined sorbent characteristics without affecting the inorganic fraction of the material, at least as far as heavy metal ions (like cadmium) are concerned.

4. Conclusions

In this work coal combustion ash (CCA) was used, either as-received or beneficiated by mechanical sieving through a 25 μm-size sieve (F25 sample) or by demineralization by acid attack (DEM sample), as cadmium sorbent from liquid solutions

at room temperature. The raw fly ash showed a significant silico-aluminous fraction and a fixed carbon content of 22% (a value observed for F25, too), while the DEM carbon content was equal to 93%. While F25 was characterized by finer particle sizes with respect to CCA, demineralization ended up in a moderate increase of the mean particle size. A ranking F25 > CCA > DEM is observable when the values of the exposed contact surface and the cumulative porosity are considered.

Cadmium adsorption kinetic tests, in good agreement with a preliminary thermodynamic characterization, revealed a satisfying cadmium uptake for all the sorbents, with maximum specific adsorption capacities ranging from 0.5 to 4.3 mg g^{-1} and following the already-noted ranking F25 > CCA > DEM. Experimental data were also interpreted in the light of either a pseudo-first-order or a pseudo-second-order kinetic model, highlighting the need of considering different models for low and high surface coverage. The first-order model was applied for far-from-saturation conditions, the second-order model for longer adsorption times. No fitting of kinetic data was possible for DEM due to its very fast saturation. Specific kinetic constants on the order of 10^{-4}–10^{-3} min^{-1} and 10^{-4} g mg^{-1} min^{-1} were obtained when the first-order (Lagergren) and the second-order (Ho and McKay) kinetic model was considered, respectively. Initial adsorption rates were on the order of 10^{-3} mg g^{-1} min^{-1}. Very interestingly, the ranking F25 > CCA > DEM was still valid for these parameters. Moreover, it was shown that both external fluid-to-particle mass transfer and macropore diffusion do not affect the adsorption process, which was instead regulated by intraparticle micropore diffusion.

In conclusion, as far as heavy metal cations like cadmium are concerned, the most useful beneficiation treatments appear to be those able to improve the sorbent surface and porosity without affecting the inorganic fraction of the material. This work also highlighted the relevance of a proper adsorbent characterization in order to better interpret the adsorption behaviour of the specific sorbent. Results were obtained carrying out a thermodynamic and kinetic investigation under determined operating conditions, referring to cadmium as adsorbate and to specific adsorbents, also beneficiated by certain treatments. Further work will make reference to different pollutants and ashes beneficiated with other methods, in order to extend the qualitative meaning of the considerations reported here.

Acknowledgements

References

[1] F. Montagnaro, P. Salatino, G. Bernardo, A. Telesca, G.L. Valenti, Reuse of fly ash from a fluidized bed combustor for sulfur uptake: the role of ettringite in hydration-induced reactivation, Energy Fuel 19 (2005) 1822–1827.
[2] S. Andini, R. Cioffi, F. Colangelo, T. Grieco, F. Montagnaro, L. Santoro, Coal fly ash as raw material for the manufacture of geopolymer-based products, Waste Manage. 28 (2008) 416–423.
[3] F. Montagnaro, M. Nobili, A. Telesca, G.L. Valenti, E.J. Anthony, P. Salatino, Steam hydration-reactivation of FBC ashes for enhanced in situ desulphurization, Fuel 88 (2009) 1092–1098.
[4] M. Marroccoli, M.L. Pace, A. Telesca, G.L. Valenti, F. Montagnaro, Utilization of coal combustion ashes for the synthesis of ordinary and special cements, Combust. Sci. Technol. 182 (2010) 588–599.
[5] C.D. Woolard, J. Strong, C.R. Erasmus, Evaluation of the use of modified coal ash as a potential sorbent for organic waste streams, Appl. Geochem. 17 (2002) 1159–1164.
[6] P. Janoš, H. Buchtová, M. Rýznarová, Sorption of dyes from aqueous solutions onto fly ash, Water Res. 37 (2003) 4938–4944.
[7] Y. Zhang, Z. Lu, M.M. Maroto-Valer, J.M. Andrésen, H.H. Schobert, Comparison of high-unburned-carbon fly ashes from different combustor types and their steam activated products, Energy Fuel 17 (2003) 369–377.
[8] S. Wang, H. Wu, Environmental-benign utilisation of fly ash as low-cost adsorbents, J. Hazard. Mater. B 136 (2006) 482–501.
[9] S. Wang, Q. Ma, Z.H. Zhu, Characteristics of coal fly ash and adsorption application, Fuel 87 (2008) 3469–3473.
[10] M. Ahmaruzzaman, Role of fly ash in the removal of organic pollutants from wastewater, Energy Fuel 23 (2009) 1494–1511.
[11] T. Wigmans, Industrial aspects of production and use of activated carbons, Carbon 27 (1989) 13–22.
[12] T. Zhang, W.P. Walawender, L.T. Fan, M. Fan, D. Daugaard, R.C. Brown, Preparation of activated carbon from forest and agricultural residues through CO$_2$ activation, Chem. Eng. J. 105 (2004) 53–59.
[13] M. Seggiani, S. Vitolo, P. De Filippis, Effect of pre-oxidation on the porosity development in a heavy oil fly ash by CO$_2$ activation, Fuel 84 (2005) 1593–1596.
[14] R. Apiratikul, P. Pavasant, Sorption of Cu^{2+}, Cd^{2+}, and Pb^{2+} using modified zeolite from coal fly ash, Chem. Eng. J. 144 (2008) 245–258.
[15] R. Apak, E. Tütem, M. Hügül, J. Hizal, Heavy metal cation retention by unconventional sorbents (red muds and fly ashes), Water Res. 32 (1998) 430–440.
[16] J. Ayala, F. Blanco, P. García, P. Rodriguez, J. Sancho, Asturian fly ash as a heavy metals removal material, Fuel 77 (1998) 1147–1154.
[17] B. Bayat, Combined removal of zinc (II) and cadmium (II) from aqueous solutions by adsorption onto high-calcium Turkish fly ash, Water Air Soil Pollut. 136 (2002) 69–92.
[18] S. Andini, R. Cioffi, F. Montagnaro, F. Pisciotta, L. Santoro, Simultaneous adsorption of chlorophenol and heavy metal ions on organophilic bentonite, Appl. Clay Sci. 31 (2006) 126–133.
[19] F. Di Natale, A. Lancia, A. Molino, M. Di Natale, D. Karatza, D. Musmarra, Capture of mercury ions by natural and industrial materials, J. Hazard. Mater. B 132 (2006) 220–225.
[20] V.C. Srivastava, I.D. Mall, I.M. Mishra, Equilibrium modelling of single and binary adsorption of cadmium and nickel onto bagasse fly ash, Chem. Eng. J. 117 (2006) 79–91.
[21] Y. Bulut, Z. Tez, Adsorption studies on ground shells of hazelnut and almond, J. Hazard. Mater. 149 (2007) 35–41.
[22] F. Di Natale, A. Lancia, A. Molino, D. Musmarra, Removal of chromium ions from aqueous solutions by adsorption on activated carbon and char, J. Hazard. Mater. 145 (2007) 381–390.
[23] A. Papandreou, C.J. Stournaras, D. Panias, Copper and cadmium adsorption on pellets made from fired coal fly ash, J. Hazard. Mater. 148 (2007) 538–547.
[24] A.B. Pérez-Marín, V. Meseguer Zapata, J.F. Ortuño, M. Aguilar, J. Sáez, M. Lloréns, Removal of cadmium from aqueous solutions by adsorption onto orange waste, J. Hazard. Mater. B 139 (2007) 122–131.
[25] K.G. Bhattacharyya, S.S. Gupta, Adsorption of a few heavy metals on natural and modified kaolinite and montmorillonite: a review, Adv. Colloid Interface Sci. 140 (2008) 114–131.
[26] A. Demirbas, Heavy metal adsorption onto agro-based waste materials: a review, J. Hazard. Mater. 157 (2008) 220–229.
[27] F. Di Natale, M. Di Natale, R. Greco, A. Lancia, C. Laudante, D. Musmarra, Groundwater protection from cadmium contamination by permeable reactive barriers, J. Hazard. Mater. 160 (2008) 428–434.
[28] F. Di Natale, A. Erto, A. Lancia, D. Musmarra, A descriptive model for metallic ions adsorption from aqueous solutions onto activated carbons, J. Hazard. Mater. 169 (2009) 360–369.
[29] S. Mohan, R. Gandhimathi, Removal of heavy metal ions from municipal solid waste leachate using coal fly ash as an adsorbent, J. Hazard. Mater. 169 (2009) 351–359.
[30] F. Montagnaro, L. Santoro, Reuse of coal combustion ashes as dyes and heavy metal adsorbents: effect of sieving and demineralization on waste properties and adsorption capacity, Chem. Eng. J. 150 (2009) 174–180.
[31] M. Balsamo, F. Di Natale, A. Erto, A. Lancia, F. Montagnaro, L. Santoro, Arsenate removal from synthetic wastewater by adsorption onto fly ash, Desalination 263 (2010) 58–63.
[32] P. Caramuscio, L. De Stefano, M. Seggiani, S. Vitolo, P. Narducci, Preparation of activated carbons from heavy-oil fly ashes, Waste Manage. 23 (2003) 345–351.
[33] Y.S. Ho, G. McKay, Sorption of dye from aqueous solution by peat, Chem. Eng. J. 70 (1998) 115–124.
[34] Y.S. Ho, G. McKay, Pseudo-second order model for sorption processes, Process Biochem. 34 (1999) 451–465.
[35] D.M. Ruthven, Principles of Adsorption and Adsorption Processes, Wiley, 1984.
[36] H.S. Harned, B.B. Owen, The Physical Chemistry of Electrolytic Solutions, ACS, 1950.
[37] R.H. Perry, D.W. Green, Perry's Chemical Engineers' Handbook, McGraw-Hill, 1997.
[38] N. Wakao, J.M. Smith, Diffusion in catalyst pellets, Chem. Eng. Sci. 17 (1962) 825–834.
[39] E.M. Tanguep Njiokep, H. Mehrer, Diffusion of ^{22}Na and ^{45}Ca and ionic conduction in two standard soda-lime glasses, Solid State Ionics 177 (2006) 2839–2844.
[40] D. Reichenberg, Properties of ion-exchange resins in relation to their structure. III. Kinetics of exchange, J. Am. Chem. Soc. 75 (1953) 589–597.
[41] R. Krishna Prasad, S.N. Srivastava, Sorption of distillery spent wash onto fly ash: kinetics and mass transfer studies, Chem. Eng. J. 146 (2009) 90–97.
[42] V.C. Srivastava, I.D. Mall, I.M. Mishra, Adsorption thermodynamics and isosteric heat of adsorption of toxic metal ions onto bagasse fly ash (BFA) and rice husk ash (RHA), Chem. Eng. J. 132 (2007) 267–278.

[43] H. Du, C.T. Williams, A.D. Ebner, J.A. Ritter, In situ FTIR spectroscopic analysis of carbonate transformations during adsorption and desorption of CO_2 in K-promoted HTlc, Chem. Mater. 22 (2010) 3519–3526.

[44] V. Gomez-Serrano, J. Pastor-Villegas, A. Perez-Florindo, C. Duran-Valle, C. Valenzuela-Calahorro, FT-IR study of rockrose and of char and activated carbon, J. Anal. Appl. Pyrol. 36 (1996) 71–80.

[45] M. Criado, A. Fernández-Jiménez, A. Palomo, Alkali activation of fly ash: effect of the SiO_2/Na_2O ratio. Part I: FTIR study, Micropor. Mesopor. Mater. 106 (2007) 180–191.

[46] V.K. Gupta, I. Ali, Removal of lead and chromium from wastewater using bagasse fly ash—a sugar industry waste, J. Colloid Interface Sci. 271 (2004) 321–328.

[47] C. Zhu, Z. Luan, Y. Wang, X. Shan, Removal of cadmium from aqueous solutions by adsorption on granular red mud (GRM), Sep. Purif. Technol. 57 (2007) 161–169.

[48] T.C. Hsu, Experimental assessment of adsorption of Cu^{2+} and Ni^{2+} from aqueous solution by oyster shell powder, J. Hazard. Mater. 171 (2009) 995–1000.